63-3-3

403 365

THE EFFECTS OF ATMOSPHERIC TURBULENCE UPON FLIGHT AT LOW ALTITUDE AND HIGH SPEED

FLIGHT RESEARCH DEPARTMENT

FDM No. 325

31 October 1961

CORNELL AERONAUTICAL LABORATORY, INC.

OF CORNELL UNIVERSITY, BUFFALO 21, N. Y.

CORNELL AERONAUTICAL LABORATORY, INC.
Flight Research Department

FDM No. 325
31 October 1961
Y

TO: W. O. Breuhaus

FROM: C. B. Notess

APPROVED: J. M. Schuler

SUBJECT: The Effects of Atmospheric Turbulence upon Flight at Low Altitude and High Speed.

TABLE OF CONTENTS

LIST OF ILLUSTRATIONS

INTRODUCTION

During the past few years, a considerable amount of information has been collected about the existence of atmospheric turbulence at low altitudes (under 1,000 feet above the terrain) and about the effects of turbulence upon the motions of an aircraft (References 1 - 5). The data indicates that during flight over land at low altitudes one can expect to encounter turbulence with an over-all probability of at least 50%.

A number of important aspects related to the problem of flight through turbulent air will be discussed herein. The first aspect to be considered is the sensitivity of a particular aircraft to turbulence. Performance requirements of the aircraft (speed and range, etc.) govern the aspect ratio and wing loading which directly influence the sensitivity of the aircraft to gust disturbances. A second aspect considered is the probability of encountering turbulence of various intensitites during low level flight operations. The third aspect is the effect of turbulence-induced vibrations on the comfort and task performance capabilities of the crew. The fourth aspect is the alleviation of turbulence-induced vibrations and loads.

CHAPTER 1

AIRCRAFT PERFORMANCE REQUIREMENTS FOR LOW ALTITUDE FLIGHT

Generally speaking, one might say that the success of manned aircraft penetrations over enemy-held territory is enhanced considerably by high speed flight at minimal altitudes; flight wherein some function of the ratio (speed/terrain clearance) is maximized. To give the pilot a good opportunity to provide on the spot mission guidance and planning, especially during surveillance missions, his maneuver capability must be great enough to enable rapid, small radius turns without excessive loss in speed. Thus a 7 g aircraft with $M \gtrsim .9$ capability is indicated as representative. At the high dynamic pressures associated with low-altitude high-speed flight, it is possible to achieve $M = .9$ and yet have reasonable maneuverability with aspect ratios less than three. However, there are other requirements such as loiter, maneuverability at low dynamic pressure (low speed and/or high altitude) and long range; all of which tend to require aspect ratios higher than three—aspect ratios as high as five.

If the above considerations are translated into an aircraft configuration which will satisfy the requirements of high maneuverability and reasonable range, the result is an aircraft of aspect ratio similar to that of the A2F which has an aspect ratio of five and wing loadings at the target of the order 75 lbs per square foot.

An alternative solution to the problem is that of an aircraft having variable sweep. For flight in the regime of low or moderate dynamic pressure, the wings would be swept forward to increase aspect ratio and thus the over-all flight efficiency as far as fuel consumption is concerned. For flight at high dynamic pressures ($M \gtrsim 0.9$ at sea level), the wings would be swept back to decrease the aspect ratio and over-all aerodynamic drag.

In the following section we will see how the mission requirements, acting through the airspeed, aspect ratio and wing loading, influence the sensitivity of an aircraft to gust-induced motions.

CHAPTER 2

THE RESPONSE OF AN AIRCRAFT TO ATMOSPHERIC TURBULENCE

When an aircraft encounters turbulence, it responds primarily by pitching, heaving, rolling and yawing. The roll and yaw occur primarily at the Dutch roll frequency of the aircraft, which is usually less than .3 cycles per second. The Dutch roll mode is often poorly damped with damping ratios less than 30% of critical. During high g maneuvers the damping of the Dutch roll mode decreases further. It is common for pilots to report that it becomes very difficult to control the sideslip and bank of an aircraft at M = .9 and 500 feet during high g turns.

In many cases the problem of lateral control can be alleviated by use of the automatic roll and yaw dampers which are standard equipment in many current aircraft. However, more sophisticated lateral autopilots may be required during high-speed low-altitude maneuvering flight. Further discussion of the lateral control problem is beyond the scope of this paper which has as its primary concern the problem of pitching and heaving.

Upon encounter with a sharp vertical gust, the inherent static stability of the aircraft will cause it to weathervane into the gust and to heave with the gust. This motion is related to the short period mode of response which usually has a natural frequency of .4 to 1.2 cps and reasonable damping during high-speed low-altitude flight. Fore and aft accelerations of a few tenths of a g can result from vertical gusts. However, these become annoying and are noticed by the pilot only in severe turbulence.

The dynamic characteristics of most types of aircraft are predetermined to a large extent by handling qualities requirements as evaluated by pilot opinion evaluations. For this reason, aircraft configurations which would satisfy the general mission requirements associated with surveillance and intrusion missions at low altitudes will not depart much in short period dynamics from the range mentioned; namely, a natural frequency of .4 to 1.2 cps with reasonable damping, $\zeta \approx .3$.

The most important and most variable factor, among different aircraft, is the sensitivity of a specific aircraft configuration to gusts. Experience indicates that if two aircraft of similar configuration fly side by side through atmospheric turbulence at the same airspeed, one aircraft may shake the pilot intolerably while the shaking of the other can be quite acceptable. It is common knowledge that aspect ratio and wing loading greatly influence the sensitivity of an aircraft to gusts. This sensitivity can be represented as the ratio of rms acceleration ($\sigma_{\Delta n_z}$) to rms vertical gust velocity (σ_{w_g}). The ratio can be estimated by use of the following equation, which is described in more detail in Appendix A.

$$S_1 = \frac{\sigma_{\Delta n_z}}{\sigma_{w_g}} = K_1 \frac{C_{L_\alpha} \rho V}{2\, W/S} \quad \text{IN } g \Big/ \frac{ft}{sec} \tag{1}$$

where C_{L_α} is the lift curve slope per radian, a function of aspect ratio

W/S is the wing loading in lb/ft^2

ρ is the air density = .0023 slugs/ft^3 at 1,000 ft MSL

V is the aircraft velocity in ft/sec

K_1 is a constant usually between the values of .60 and .90 at low altitude, which takes into account the dynamic characteristics of the aircraft and the gust input spectrum

Equation 1 indicates that S_1 increases directly proportional to C_{L_α} and airspeed, and decreases as wing loading increases and as altitude increases. Recent flight experience through thunderstorms illustrates that at supersonic speeds, the intensity of shaking is relatively insensitive to airspeed changes (Reference 6). This is primarily a result of the fact that $C_{L_\alpha} V$ remains essentially constant for Mach numbers greater than 1.10.

The above equation is similar to the familiar Derived Gust Equation used to convert peak values of acceleration measured on VGH recorders to equivalent peak gust velocity (Reference 3). The only difference is the value of the constant K_1. The above equation is also similar to the equation for $\bar{A}_1$ described in Reference 7. In this case K_1 is similar to the gust response factor $\sqrt{\frac{I(K, A)}{\pi}}$.

It can be shown that the pitching motion induced by gusts is so phased in relation to the acceleration induced by gusts that the cockpit, well forward of cg, will experience as much as 15% less acceleration than the cg at the short period frequency. Thus the factor K_1 will be decreased as the distance of the cockpit forward of the cg increases. For large flexible airframes the structural modes will act to increase K_1 slightly, by contributing vibration energy at frequencies greater than 2 cps. The important effect of these vibrations will be discussed in a later section. Another important factor included in K_1 is the effect of the short period natural frequency, f_n of the aircraft, which can vary from .4 cps to 1.2 cps as the aircraft inertia decreases relative to the wing loading. Since the intensity of turbulence decreases with increasing gust frequency (decreasing wavelength), it can be shown that K_1 is roughly proportional to $\frac{1}{\sqrt{f_n}}$ where f_n is the short period resonance defined at some constant Mach No. The numerical value of K_1 chosen for presentation herein is .67. Typical values of K_1 at the cg for several aircraft, computed from rms Δn_z and rms w_g data obtained from integration of spectra are shown in Table 1.

TABLE 1

TYPICAL VALUES OF K_1 AND $\sqrt{\frac{I(K,\omega)}{\pi}}$

FH-1 at M = .4	K_1 = .59	$\sqrt{\frac{I(K,\omega)}{\pi}}$ = .53
A2F at M = .60 and .85	K_1 = .61	$\sqrt{\frac{I(K,\omega)}{\pi}}$ = .59
B-66 at M = .51	K_1 = .81	$\sqrt{\frac{I(K,\omega)}{\pi}}$ = .65

Figure 1 shows lines of constant sensitivity, S_1, as determined for various wing loadings (W/S the ordinate) and various lift curve slopes (C_{L_α}, the abscissa) at M = .9 and an altitude of 1,000 feet above mean sea level. A value of K_1 = .67 was selected as being representative.

Figures 2 and 3 show similar plots at M = .6 and M = .9 with K_1 = .67. For illustrative purposes several current aircraft have been located on the plots on the basis of an approximate wing loading while halfway through the mission, and an estimated C_{L_α}. The C_{L_α} values were estimated from planform data when wind tunnel experiments were not available. It should be emphasized here that wing loadings can vary as much as 50% between take-off and landing, due to expenditure of fuel and weapons; hence Figures 2 and 3 illustrate only qualitative information concerning S_1, rather than exact information. If the actual value of K_1 is other than .67 for any specific aircraft, the S_1 values obtained from Figures 2 and 3 should be modified accordingly.

On the basis of the information presented in Figures 2 and 3, one perhaps can generalize and state that low aspect ratio supersonic configurations, when flying at M = .9 at low altitude, are least sensitive to turbulence. However, these aircraft being supersonic designs have inherently poor performance (limited range) at such flight conditions. The A2F to some extent represents an aircraft specifically designed to perform at low levels and high speeds. It is seen that the A2F is considerably more gust sensitive than the B-58. At M = .9 the B-58 has a sensitivity to turbulence which is about half that for the A2F.

CHAPTER 3

PROBABILITY OF ENCOUNTERING TURBULENCE AT LOW ALTITUDES

Turbulence at low altitudes above theterrain is the result of complex interactions between a number of meteorological factors, the foremost of which are unstable temperature lapse rates and the presence of winds. References 8 and 9 present summaries of the situation.

A considerable amount of data has been collected about atmospheric turbulence at low altitudes. (See References 1 through 5 and 19). Much of the data represents measurement of peak vertical accelerations and, by use of an equation similar in form to Equation 1, conversion to the corresponding peak gust data. Figure 4 shows a number of curves relating peak gust velocity to probability of occurrrence. The curve for 500 feet was estimated by considering recent data at altitudes under 1,000 feet. This curve roughly agrees with the modifications to data in Reference 2 which are implied by MIL-A-8866. (Reference 10).

Data obtained under recent programs such as those using the B-66 and the FH-1 (References 1 and 4) have presented the data in the form of rms gust velocity rather than peak counts. Harry Press of the NASA (Reference 7) has described techniques for relating peak count data to rms data. These two types of data can be related in another way which enables a simple application to the specific problem at hand. Data from References 1 and 4 was analyzed and indicates that on the average a gust of extreme magnitude is usually associated with a nearly homogeneous patch of turbulence having an rms of one-fourth the extreme value in an extent of ten miles. Thus, it is reasonable to assume that in every flight there will be at least one patch of turbulence (10 miles) which is associated with the peak gust encountered and which will have an rms gust velocity equal to one-fourth of this peak value. The foregoing is described in more detail in Appendix C.

The "Estimated" curve in Figure 4 indicates that one might expect to encounter a derived gust velocity peak exceeding 20 ft/sec once for every 100 miles of flight. This implies that on the average at least one patch of turbulence, ten miles long, would be expected during 100 miles of flight with an rms value of 20/4 = 5 ft/sec. In other words the probability of being in a patch of turbulence with $\sigma_{w_g} \geqq 5$ fps is 10%; or the probability of encountering turbulence with $\sigma_{w_g} \geqq 5$ fps is 10%.

It is important to realize that the above are statistical probabilities. The encounter of a peak gust of 20 ft/sec on the average of once every one hundred miles is based upon thousands of miles of sampled data. Therefore, the 10% probability of finding a patch of turbulence with an rms exceeding 5 ft/sec should not be applied to any particular flight of 100 or 200 miles. It is more accurate to say that if several random flights are considered which together involve a total of at least 1,000 miles, then 10% of this distance may be expected to contain turbulence having a $\sigma_{w_g} \geqq 5$ fps.

A probability distribution of σ_{w_g} is plotted in Figure 5 as the curve identified with X's. This curve was obtained as described above from the estimated peak count curve in Figure 4. Other data shown in Figure 5 indicates probabilities which are higher than the estimated curve, while the B-66 data from Reference 4 closely follows the estimated curve. The scatter is believed to be largely due to the method of evaluating the gust sensitivity factor. The factor $\bar{A}_1$ used for obtaining the two NACA curves in Figure 5 is only a rough approximation based on no freedom to pitch and tends to be lower than S_1. For the remainder of this paper a conservative compromise among the curves was used. This curve is identified with triangles in Figure 5. The probability of exceeding $\sigma_{w_g} = 5$ fps was taken to be 15%, and that for $\sigma_{w_g} = 8$ fps as 1%.

It is obvious that more data is needed in order to support more reliable estimates of the probability of encountering turbulence at low altitudes.

CHAPTER 4

VARIATION OF TURBULENCE EXPECTANCY

The probability of encountering turbulence given in the preceeding section is based upon data gathered from a number of sources. The data is insufficient to determine any variations of this probability which are associated with geographical region, time of year and time of day. The data discussed above at best represents an all-year-round average based on operating over the United States.

References 8 and 9 present interesting data on daily variations of gustiness. The predominant gustiness at low altitudes during the day is due to convective activity and wind shear. If the sky is clear, solar heating will increase convective activity during the day. Increased convection leads to mixing of winds in the vertical direction and generally decreases the wind shear. Thus, wind shear tends to be the primary factor in the generation of turbulence at night while during clear days convective activity assumes an important role.

Another important factor in the generation of turbulence is rough terrain. Winds blowing over rough terrain break up into eddies and generate "mechanical" turbulence which in some cases is observed as increased turbulent energy in the vicinity of mountain peaks. Certain types of hills and wind conditions generate mountain waves or standing waves. However, these latter special conditions are found very infrequently.

Since wind and terrain roughness are important factors in turbulence generation, it is possible to obtain general indications about geographical areas which would tend to have more intense turbulence, on the average, than other regions. For example, areas such as the Southeastern United States around Georgia are known to have relatively flat terrain and also relatively low surface winds, (Reference 8), while the Northeastern United States has hilly terrain and a higher mean wind level. Thus, in the Northeast, one would expect to encounter turbulence of greater intensity than one would expect over Georgia.

Further discussion about the variation of turbulence expectancies is beyond the scope of this paper. It is the author's guess that probabilities of encountering various levels of turbulence, which represent all-year-round averages over the United States, might increase for certain definite geographical areas by as much as a factor of 2 to 3 for mountainous-windy areas and might decrease by as much as a factor of 5 to 10 for non-windy areas.

CHAPTER 5

EFFECT OF TURBULENCE-INDUCED MOTIONS UPON THE CREW

A considerable amount of flying has been done under conditions of high speed at low altitude. References 5 and 11 represent two of the more extensive investigations. Unfortunately, however, the experimental design of much of this flight work was based on several factors, and thus is not specifically suited for the evaluation of the effects of turbulence on pilot performance. In cases where experiments were aimed at determining the effect of acceleration on the ability of the pilot to fly at M $\gtrless$ .6 and $h < 500$ feet and to stay on course while performing a variety of simple psychomotor tasks (as pushing buttons and writing, and such mental tasks as planning or checking fuel supply, noting arrival at check points, etc.), it is consistently evident that at rms levels exceeding .25 g's the pilot's task proficiency is decreased. Most of us have experienced such levels at one time or another in an airliner and would agree that the turbulence associated with an occasional 1 g peak is disturbing. In cases where the pilot had only to fly a route familiar from past flights or well studied on maps, with no definite task assignment or evaluation procedure, his opinion was that rms g levels as high as .35 were not bothersome. However, in such flights, the pilot often slowed down or increased altitude. Accurate measures of pilot work load and performance are not generally available from these flights.

The particular aspects of exposure to vibration which are of importance are the intensity of vibration, the oscillatory frequencies present in the vibration, and the duration of exposure to various intensity levels. The curves shown in Figure 6 are based upon a comparison of flight data presented in References 4, 5, and 11 and other sources. The curves show the duration of exposure to various intensity levels above which the pilot's task proficiency begins to decrease and, above which the pilot's rating is intolerable. These rms values are based on acceleration spectra having maximum energy centered near 0.8 cps. Appendix B contains a more detailed discussion related to these problems.

The frequencies of oscillation which contribute to the rms acceleration are important. In the discussion above the power spectrum of acceleration is assumed to be essentially that of a rigid aircraft with a well damped resonance at the short period frequency (.4 to 1.2 cps). In other words, fuselage bending and wing bending modes of structural vibration are not considered in Figure 6. Structural vibrations are usually of high frequency and will be discussed in detail in the next paragraph. Some analysis (Reference 12) has been performed which indicates that the high frequency vibratory accelerations can be modified to acceptable levels by using spring mounted seats for the crew members. Spring mounting cannot alleviate low frequency accelerations below the short period frequency because the displacements required become prohibitive (of the order of one to two feet). It appears that if the high frequency energy is filtered, thereby introducing a low frequency resonance (lightly damped low frequency mode), the over-all effect is an improvement—even if the rms content of the motion is not decreased. Humans in all probability can adapt themselves to sinusoidal motions (swing, see-saw, and rocking horse) easier than they can adapt to random unpredictable motions.

Figure 7 shows some experimental data which illustrates the importance of high frequency energy. Figure 7 is based upon data obtained from acceleration measurements made simultaneously upon a sprung seat and upon the cockpit bulkhead. It is evident that a spring damper system approximating two second-order filters, with f_{n_1} = 1.5 cps and f_{n_2} = 4 cps, filters out the structural vibrational energy. An observer using the seat indicated that there was considerable improvement in his ability to perform simple tasks such as reading and writing. Because of the increase in energy at low frequencies, the actual rms "g" level was slightly increased by the sprung seat.

The data from Magid, et al. (Reference 18) indicates that near one cycle/sec the tolerance boundaries follow constant $\dot{g}$ or constant jerk levels. This fact, if applied to random vibration, would imply that tolerance levels would decrease with increasing frequency according to $1/\omega^2$. Such a curve is shown in Figure 7. This curve illustrates clearly why the attenuation of energy at 4 cps improved the opinion of the observer.

CHAPTER 6

SYNTHESIS OF PRECEDING SECTIONS

It is now possible to combine the information presented above on aircraft sensitivity to gusts, probability of gust encounter and human tolerance to obtain an over-all picture of the effect of gusts on the crew.

It is reasonable to assume that if a particular flight encounters one patch of severe turbulence the meteorological and terrain features will be sufficiently wide spread so that adjacent patches of turbulence would have a high probability of containing, at least, moderate turbulence. On this basis let us assume that a typical mission involves 100 miles of low altitude flight at M = .9. In addition, another 200 miles at M = .6 are added. Table 2 indicates the rms acceleration which would have to be withstood by two representative aircraft if the rms gust velocity is 5 ft/sec.

TABLE 2

TABLE OF TWO REPRESENTATIVE EXAMPLES

Aircraft	A		B	
Aspect Ratio	2	2	5	5
Mach No.	.6	.9	.6	.9
Miles Flown at each Mach No.	200	100	200	100
Time at each Mach No. in minutes	27	9	27	9
Aircraft Sensitivity at cockpit, s, in g/fps	.018	.030	.038	.060
RMS turbulence level in fps exceeded 15% of the time	5	5	5	5
Vibration level, rms g's	.09	.15	.19	.30
Pertinent Pilot Proficiency Boundary, rms g's	.18	.22	.18	.22
Pertinent Pilot Intolerance Boundary, rms g's	.32	.43	.32	.43

The data shown in Table 2 indicates that aircraft B is roughly twice as sensitive to turbulence as is aircraft A. If one multiplies the sensitivity, S_1, by the rms gust velocity of 5 fps for each case, the rms vibration level in g's is obtained.

The pilot proficiency and tolerance data pertaining to exposures of 9 and 27 minutes was obtained from Figure 6. It is evident that aircraft A at no time exceeds the limit of pilot proficiency. In other words, the pilot can perform his duties unhampered by the level of vibration. Aircraft B vibrates at a level which is just slightly above the pilot proficiency boundary at M = .6, but significantly above the boundary at M = .9. The intolerable boundary is not reached by either aircraft.

Since the over-all probability of encountering turbulence with rms levels exceeding 5 fps is 15%, we can say that on one out of every 7 missions the pilot in aircraft B would be performing under a serious handicap due to gust-induced vibration. Aircraft A would exceed the proficiency boundaries if the rms gust intensity was increased to 8 fps. An rms gust velocity of 8 fps is exceeded with a probability of 1% or on only one out of every 100 missions. From this point of view Aircraft A, which has 1/2 the S_1 value of Aircraft B, gives the pilot an acceptable ride on a considerably greater percentage of his missions.

CHAPTER 7

GUST ALLEVIATION AND LOAD ALLEVIATION

If the performance and mission requirements for an aircraft are such as to specify a configuration which is sensitive to atmospheric turbulence, some form of automatic gust alleviation may be necessary. As soon as the wing encounters a sharp-edged gust, the aerodynamic lift changes in a few hundredths of a second producing a peak vertical acceleration. When the horizontal tail enters the gust a few hundredths of a second later, the tail lift tends to pitch the aircraft so that it weathervanes into the gust, thus alleviating the gust-induced increment to wing lift. Until the wing lift increment is thus alleviated, the lift induces a vertical acceleration which causes a build up of vertical velocity. Even if the aircraft is restrained in pitch, the heaving which results from gust-induced lift will reduce the angle of attack, thus alleviating the gust-induced acceleration as the aircraft rises with the gust.

Generally speaking, the major portion of motion energy caused by turbulence is centered around the short period resonant response of the rigid airframe, .4 to 1.2 cps. These motions can be attenuated by decreasing the sensitivity of an aircraft to gusts by inherent features of the wing planform or by providing automatic control surfaces capable of varying the aerodynamic lift forces on wing and tail.

A re-examination of Equation 1 indicates that the gust sensitivity of an aircraft can be reduced by maximizing the wing loading, by decreasing C_{L_α} or aspect ratio, and by increasing damping of the short period mode.

One type of aircraft which has been considered for the low level mission is the variable sweep aircraft which would use the benefits of higher aspect ratio during landing, take-off, high altitude cruise and maneuvers, and low altitude loiter and maneuvers. The benefits of low aspect ratio would enable supersonic maximum speed runs while simultaneously decreasing the sensitivity of the aircraft to turbulence.

It is difficult to make generalized statements concerning the over-all utility of low aspect ratios with their inherent gust alleviation capabilities. Many other factors must be considered. It has been said that the disturbances to lateral motion become relatively more serious as the aspect ratio and therefore the inertia in roll decreases.

There are certain surveillance and intrusion missions which do not require supersonic dash capabilities, and thus would be best filled by aircraft with aspect ratios near 5. Certain types of cargo and troop transports will also have high aspect ratios.

For aircraft which have aspect ratios and wing loadings which combine to provide a high gust sensitivity $S_1 \geqq .05$, it may be necessary to provide automatic gust alleviation. To alleviate the gust-induced motions, the wing lift must be attenuated in a time interval which is smaller than the short period response time of 1 to 2 seconds. This can be done only by changing the effective wing incidence either automatically by aerodynamic twisting moments or by using some other means for varying lift such as spoilers or trailing edge flaps. References 13 and 17 indicate that present-day hydraulic servo systems can move trailing edge flaps sufficiently fast to alleviate 80% or more of the gust-induced lift at a Mach No. 1.2. Generally, the use of flaps to alleviate lift and elevator to counter pitching is the most practical approach to the problem. The NASA in References 14 and 15 has achieved better than 50% alleviation by such methods.

CHAPTER 8

STRUCTURAL FATIGUE

The aerodynamic forces and moments induced by the gusts contribute to structural fatigue at the same time that they contribute to pilot fatigue. It is the airframe structure which must transfer the loads from wings and tail to the cockpit. Therefore, generally speaking, when the pilot is vibrated and shaken severely, the structural loads are also varying with significant magnitudes. During high speed flight the gusts appear as high frequency loads of moderate magnitude which consume the fatigue life of the aircraft primarily in the region of the S-N diagram defined by frequently occurring moderate to low stress oscillations.

At a speed of .9 Mach number, a 20-foot per second gust causes a change in angle of attack of 1.2 degrees. This means that 50% alleviation can be obtained by .6 degrees change of wing incidence or by about 3 degrees of flap deflection. Alleviation by means of wing twist is deeply involved with related flutter problems and therefore flap type alleviation systems have been proposed by most investigators.

The flap type system reduces wing bending and shear loads considerably, but tends to increase the wing torsion and the tail loads. However, generally speaking, the fatigue problem is reduced, since it may be relatively easy to beef up the horizontal tail. Reference 15 discusses results of load alleviation investigations by NASA with a C-45 aircraft wherein the wing bending and shear were reduced by 30%.

CONCLUSIONS

At low altitudes the probability of encountering patches of turbulence with rms vertical gust velocities exceeding 5 ft/sec is about 15%. The sensitivity to gusts of current aircraft flying at M = .9 can vary from .03 to .07 (g's per ft/sec) of rms gust velocity. Typical long range, maneuverable high speed aircraft fall approximately in the region (.04 to .05 "g's" per fps), and therefore the pilot can expect to be shaken at an rms "g" level of about .25 "g" on 15% of his low level dash missions.

An rms "g" level of .25 corresponds to occasional 1 "g" peak jolts. After several minutes of exposure to such intensity levels, the pilot becomes handicapped in performance of his tasks.

Gust alleviation by use of trailing edge flaps or variable sweep can provide the pilot with a comfortable ride allowing him to function efficiently, while simultaneously reducing the problem of structural fatigue accumulation due to repeated gust loads.

LIST OF REFERENCES

1. Notess, C.: Analysis of Turbulence Data Measured in Flight at Altitudes Up to 1600 Feet Above Three Different Types of Terrain. CAL Report No. TE-1215-F-1, February 1959.

2. Press, H. and Steiner, R.: An Approach to the Problem of Estimating Severe and Repeated Gust Loads for Missile Operations. NACA TN 4332, September 1958.

3. Walker, W. and Copp, M.: Summary of VGH and V-G Data Obtained From Piston-Engine Transport Airplanes from 1947 to 1958. NASA TN D-29, September 1959.

4. Douglas Aircraft Company, Inc.: B-66B Low Level Gust Study. WADD TR 60-305, 1961.

5. Army Aviation Board–Report of Project NR AVN 4860–Man-Machine Environment Compatibility Studies and Tests in Support of Surveillance Aircraft Development. Ft. Rucker, Alabama, March 1961, ASTIA Doc. AD. 249956.

6. Roys, G.: Thunderstorm Penetrations by an F-106A Aircraft at High Speed and High Altitude. WADD TB 60-274, December 1960.

7. Press, H.; Meadows, M.; and Hadlock, I.: A Reevaluation of Data on Atmospheric Turbulence and Airplane Gust Loads for Application in Spectral Calculations. NACA TR 1272, 1956.

8. United States Air Force, Air Force Cambridge Research Center: Handbook of Geophysics for Air Force Designers. 1960.

9. Singer, Irving and Raynor, Gilbert: Analysis of Meteorological Tower Data April 1950–March 1952 Brookhaven National Laboratory. AFCRC-TR-57-220, ASTIA Document No. AD 133806, 1957.

10. Military Specification–Airplane Strength and Rigidity Reliability Requirements, Repeated Loads, and Fatigue. MIL-A-8866 (ASG), 18 May 1960.

11. Kerr, T. H. and Nethaway, J. E.: An Investigation into the Problems of Flying an Aircraft at High Subsonic Speed at Very Low Altitude. Technical Note No. Aero. 2714, Royal Aircraft Establishment, August 1960. (Title Unclassified, Report SECRET).

12. Notess, C. B.: A New Look at Gust Alleviation. Cornell Aeronautical Laboratory, Inc. FDM No. 314, December 1960 (CONFIDENTIAL)

13. Notess, C. and Jagger, D.: On the Feasibility of an Adequate, Fast Response, Gust Alleviation System. Cornell Aeronautical Laboratory, Inc. FDM No. 300, September 1959.

14. Hunter, P.; Kraft, C.; and Alford, W.: A Flight Investigation of an Automatic Gust-Alleviation System in a Transport Airplane. NASA TN D-532, 1961.

15. Schott, R. and Hamer, H.: Flight Investigation of Some Effects of a Vane-Controlled Gust-Alleviation System on the Wing and Tail Loads of a Transport Airplane. NASA TN D-643.

16. Goldman, D. and Von Gierke, H.: The Effects of Shock and Vibrations on Man. Naval Medical Research Institute, Bethesda, Maryland, Lecture and Review Series No. 60-3, 1960.

17. Notess, C.: A Gust Alleviator System Which Does Not Affect the Normal Flight Characteristics or Maneuverability. CAL FDM No. 305, December 1959.

18. Magid, et al: Human Tolerance to Whole Body Sinusoidal Vibration. Aerospace Medicine, November 1960.

19. Zbrozek, J. K.: The Relationship Between the Discrete Gust and Power Spectra Presentations of Atmospheric Turbulence, with a Suggested Model of Low-Altitude Turbulence. London: Her Majesty's Stationery Office. R. & M. No. 3216, 1961.

FIGURE 1: GUST SENSITIVITY

M = .90 AT 1000 FT. ABOVE MSL

$K_1 = .67$, $\omega_{sp} = .8$ CPS

$S_1 = \sigma_{\Delta n_z} / \sigma_{\alpha g} \sim g/FPS$

$S_1 = K_1 \dfrac{C_{L\alpha} \rho V}{2\, W/S}$

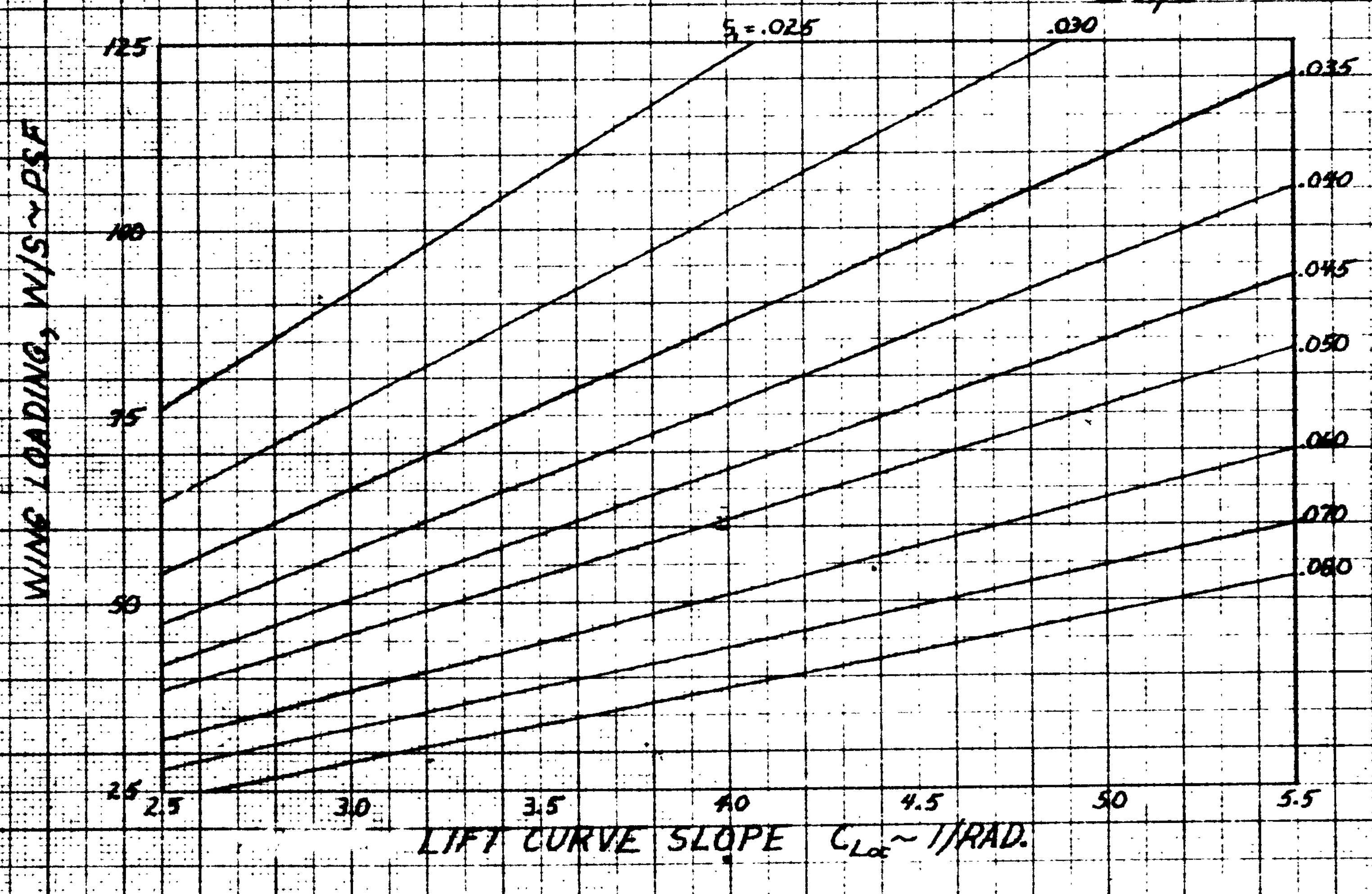

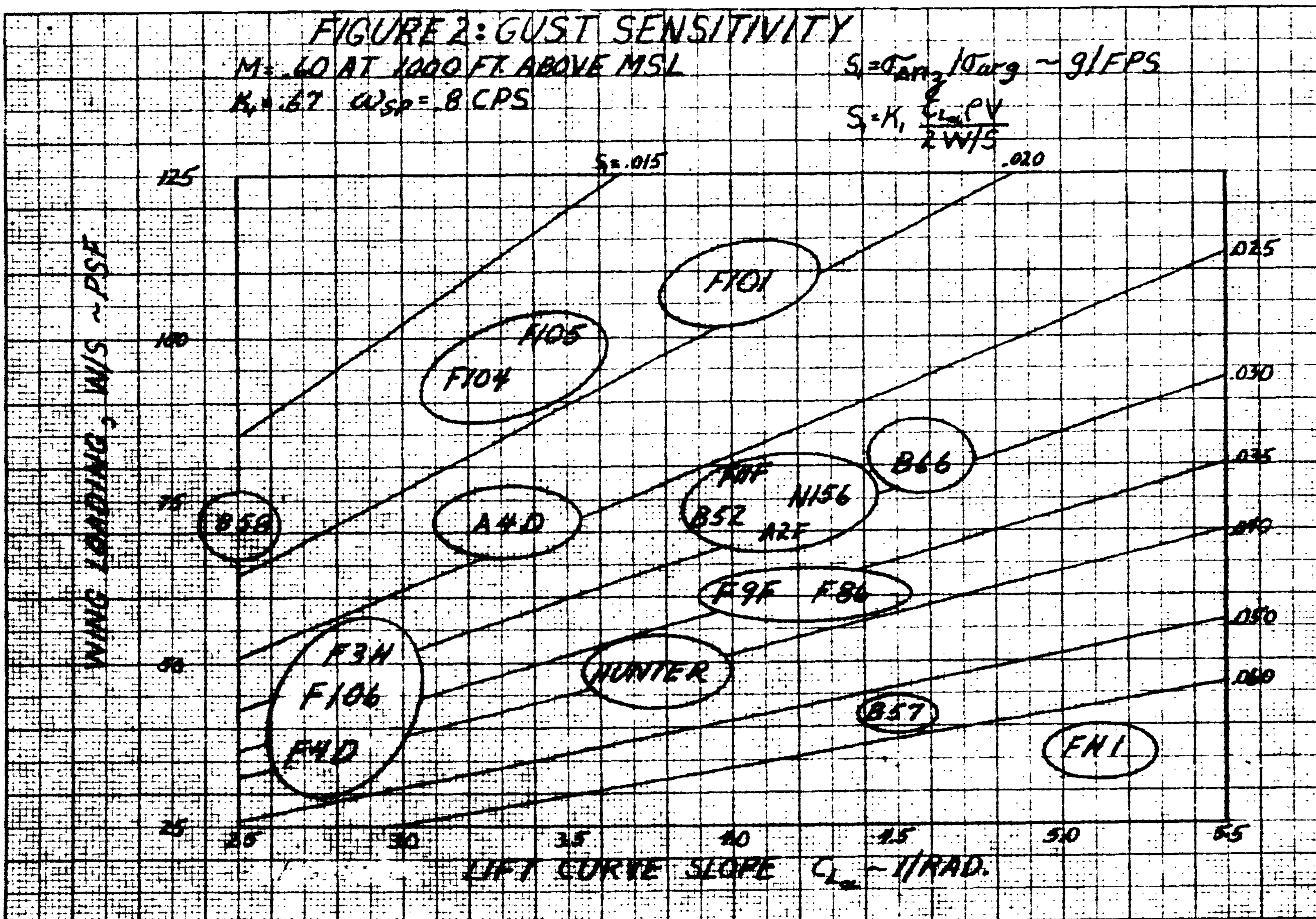

FIGURE 2: GUST SENSITIVITY

FIGURE 3: GUST SENSITIVITY

M=.90 AT 1000 FT. ABOVE MSL

K_1=.67, ω_{sp}=.8 CPS

$S_1 = \sigma_{\Delta n_z} / \sigma_{w_g} \sim g/FPS.$

$S_1 = K_1 \cdot \frac{C_{L_\alpha} \rho V}{2\, W/S}$

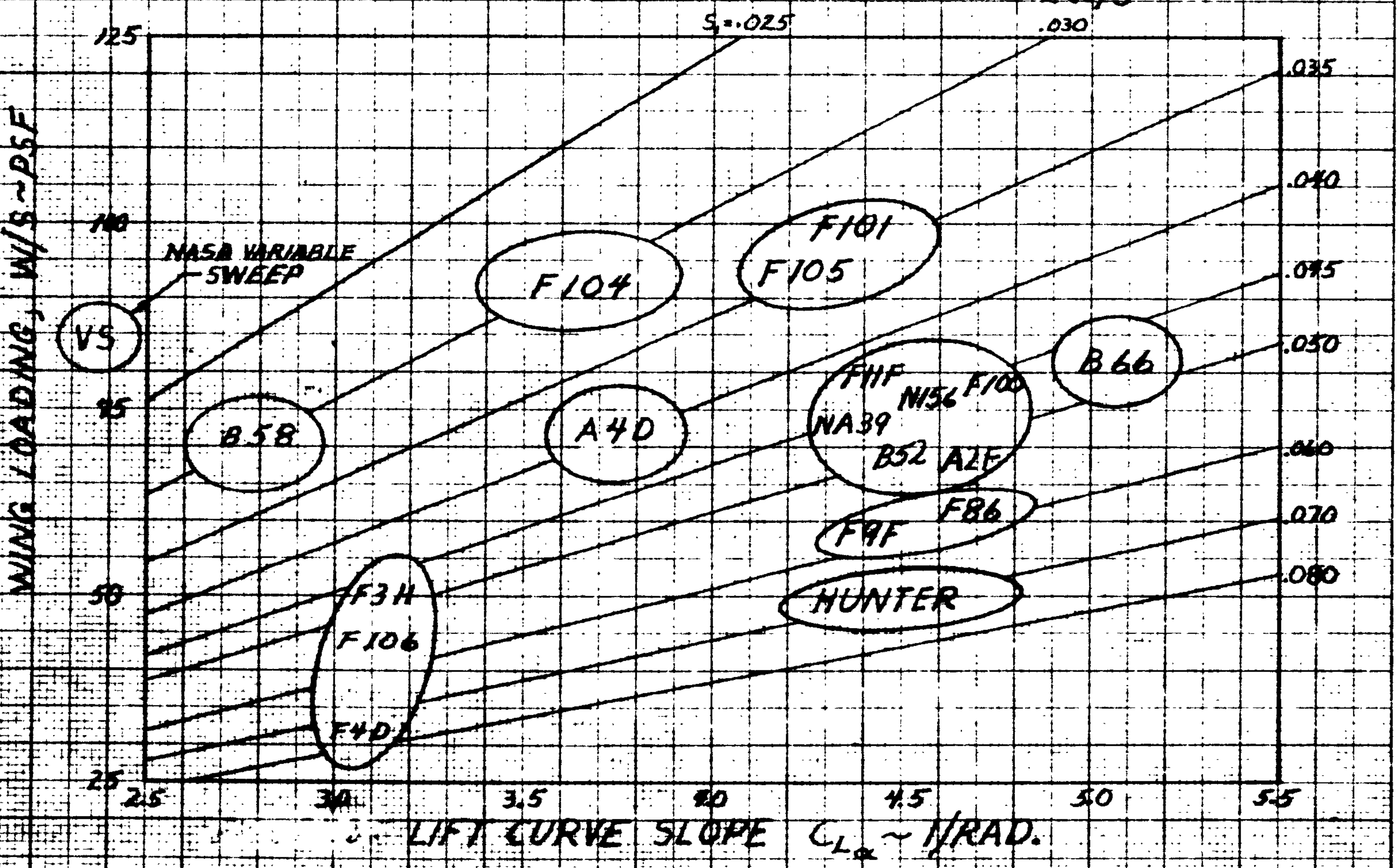

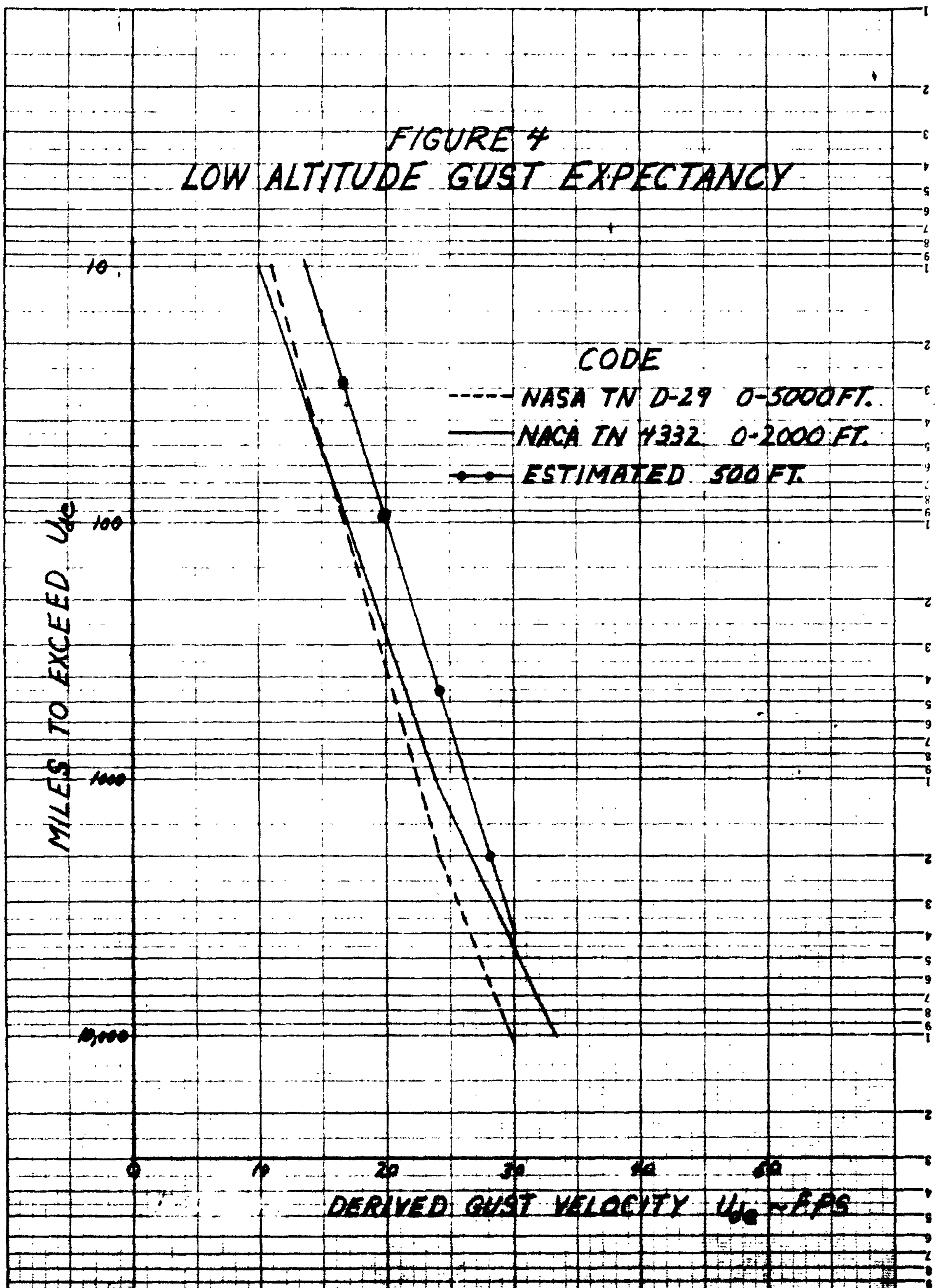
FIGURE 4
LOW ALTITUDE GUST EXPECTANCY
CODE
NASA TN D-29 0-5000 FT.
NACA TN 4332 0-2000 FT.
ESTIMATED 500 FT.
MILES TO EXCEED U_{de}
10
100
1000
10,000
0
10
20
30
40
50
DERIVED GUST VELOCITY U_{de} ~ FPS

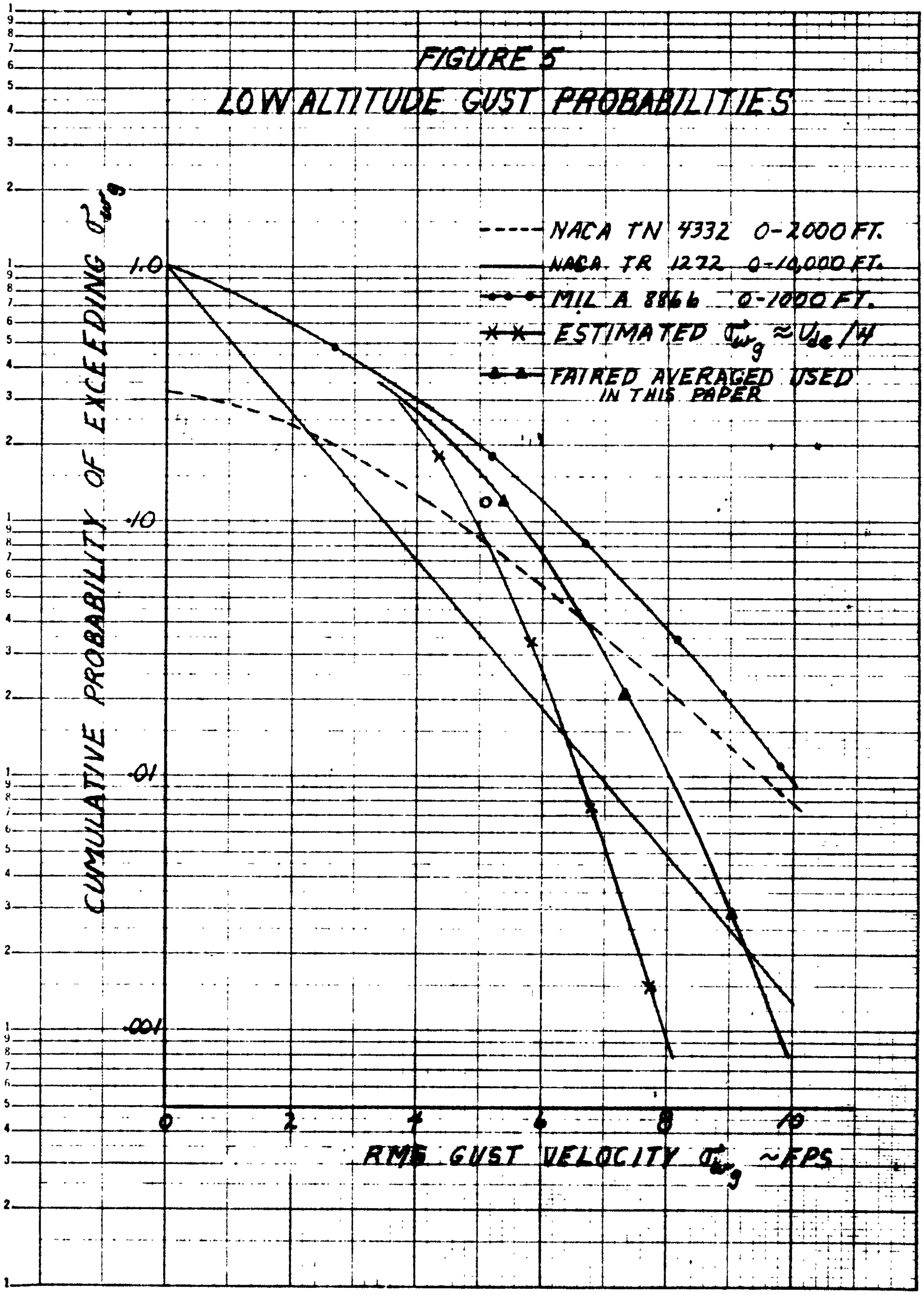
FIGURE 5
LOW ALTITUDE GUST PROBABILITIES
NACA TN 4332 0-2000 FT.
NACA TR 1272 0-10,000 FT.
MIL A 8866 0-1000 FT.
ESTIMATED $\sigma_{w_g} \approx U_{de}/4$
FAIRED AVERAGED USED IN THIS PAPER
CUMULATIVE PROBABILITY OF EXCEEDING σ_{w_g}
1.0
.10
.01
.001
0
2
4
6
8
10
RMS GUST VELOCITY σ_{w_g} ~FPS

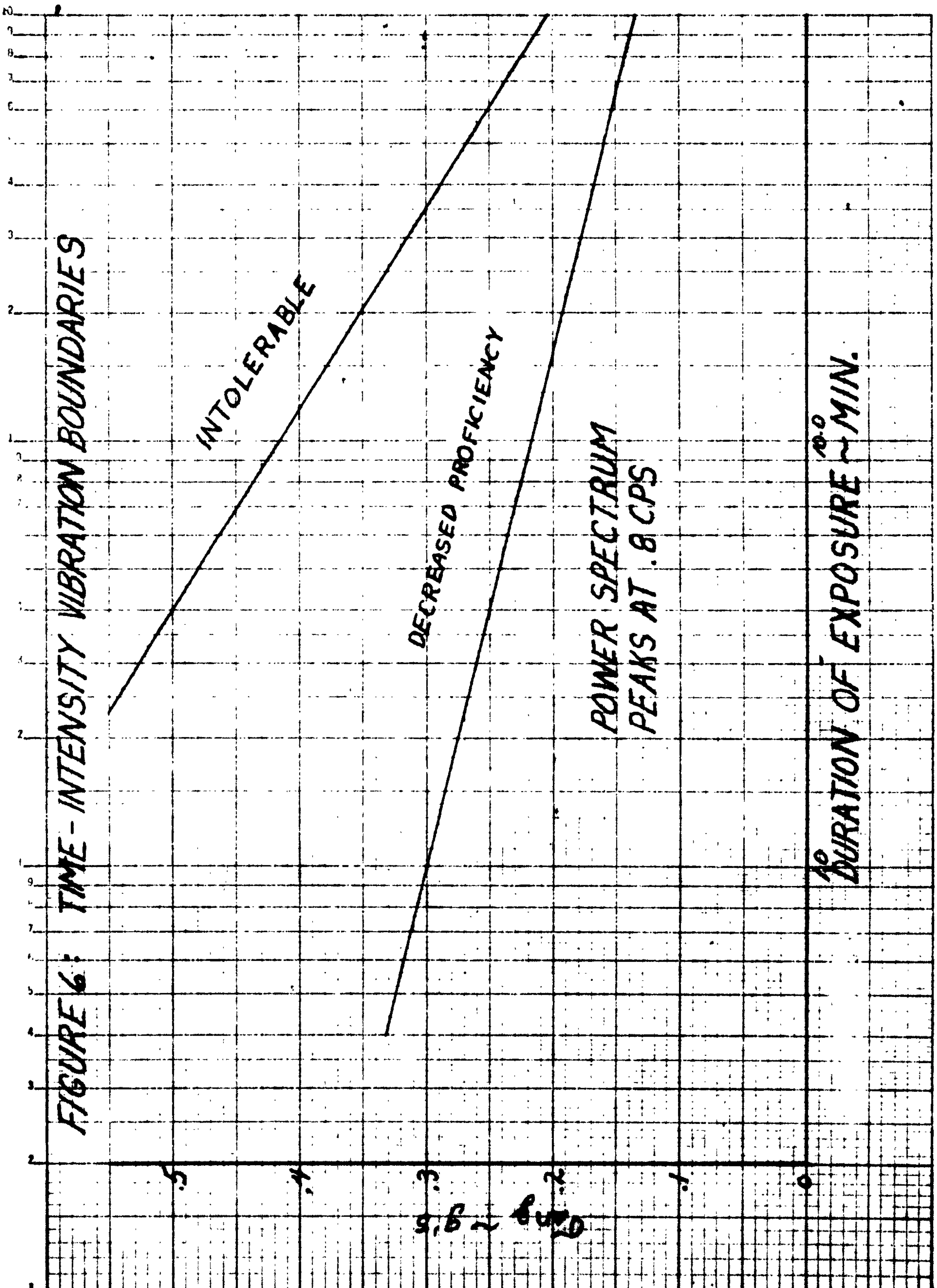

FIGURE 6: TIME-INTENSITY VIBRATION BOUNDARIES

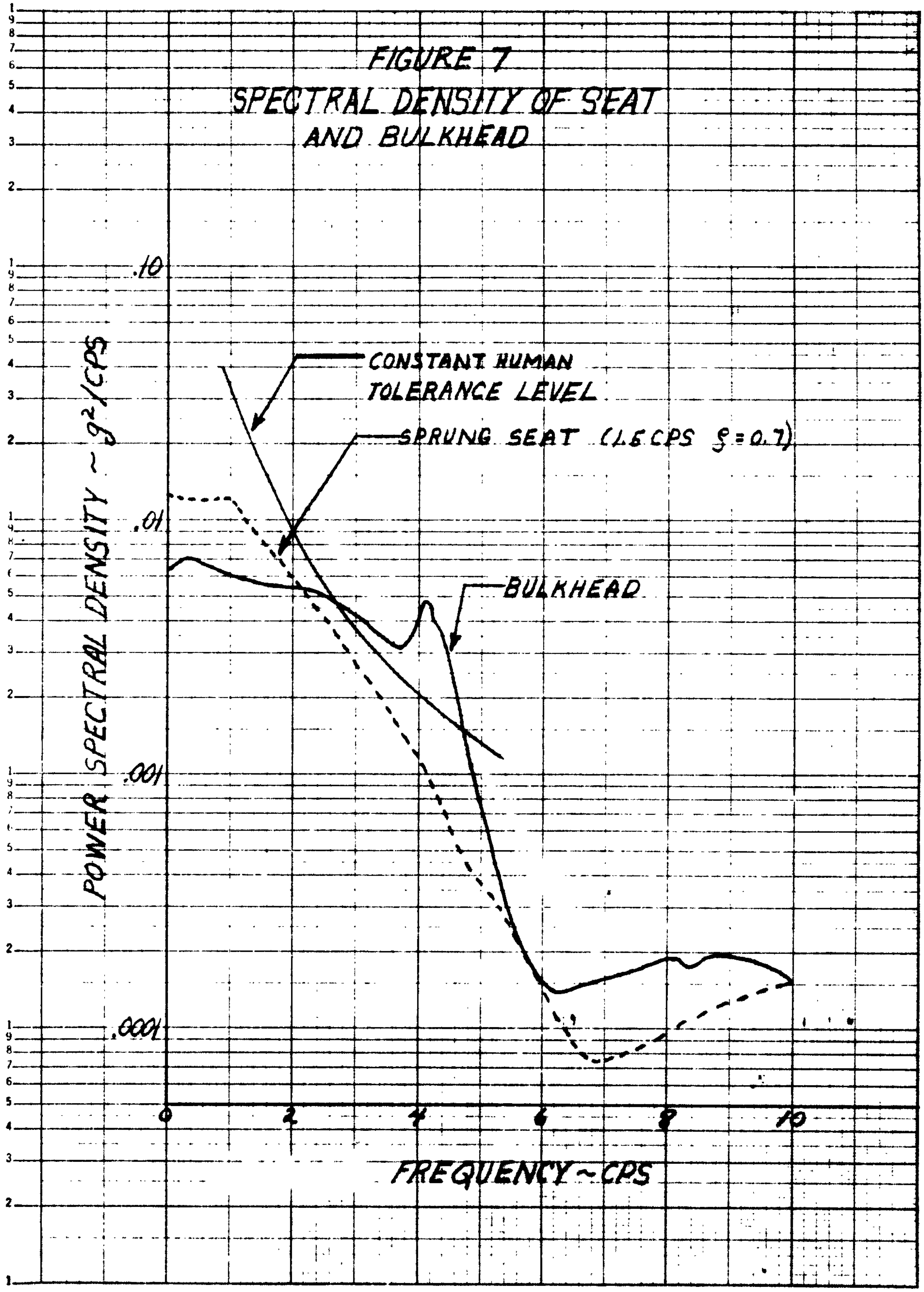
FIGURE 7
SPECTRAL DENSITY OF SEAT
AND BULKHEAD
CONSTANT HUMAN
TOLERANCE LEVEL
SPRUNG SEAT (1.6 CPS ς=0.7)
BULKHEAD
POWER SPECTRAL DENSITY ~ g²/CPS
.10
.01
.001
.0001
0
2
4
6
8
10
FREQUENCY ~ CPS

APPENDIX A

GENERALIZED GUST RESPONSE OF AN AIRCRAFT

The following is a derivation of an approximate method for estimating the sensitivity of an aircraft to gusts during high-speed low altitude flight. The sensitivity is expressed in the form rms normal acceleration per unit rms vertical gust velocity.

The transfer function relating gust-induced vertical acceleration at the cg of an aircraft to vertical gust velocity can be obtained by writing two degree-of-freedom equations of motion (pitch and vertical acceleration) and solving for the transfer function $\Delta n_z / w_g$. The result is as follows:

$$\frac{\Delta n_z}{w_g} = -\frac{C_{L_\alpha} \rho V}{2\, W/S} \quad \frac{d\left(d - M_{\dot\theta}/I_y\right)}{d^2 + 2\zeta\omega_n d + \omega_n^2} \qquad \text{A-1}$$

where $\frac{\Delta n_z}{w_g}$ is the incremental acceleration at the cg per unit vertical gust velocity, g per ft/sec

C_{L_α} is lift curve slope per radian

ρ is air density in slugs/ft^3

V is airspeed in ft/sec

W/S is wing loading [weight/wing area], lbs/ft^2

ζ is damping ratio of short period mode

ω_n is natural frequency of short period mode, rad/sec

$M_{\dot\theta}$ is damping in pitch, $\partial M/\partial \dot\theta$, foot-lbs/rad/sec

I_y is moment of inertia in pitch, slug-ft^2.

d is the operator replacing d/dt

For present day aircraft, ω_n is usually found to lie in the frequency range 3–7 radians per second. Large bombers tend to have low values of ω_n near 3 radians per second, and fighters flying at transonic speeds are at the high end, near 7 radians per second. The damping ratio ζ is usually between .3 and .5 of critical. If structural modes are considered in the determination of the transfer function, resonant peaks will occur at the higher frequencies associated with the structural modes; however since these resonances contribute negligible amounts to the total rms "g's", they will not be considered herein.

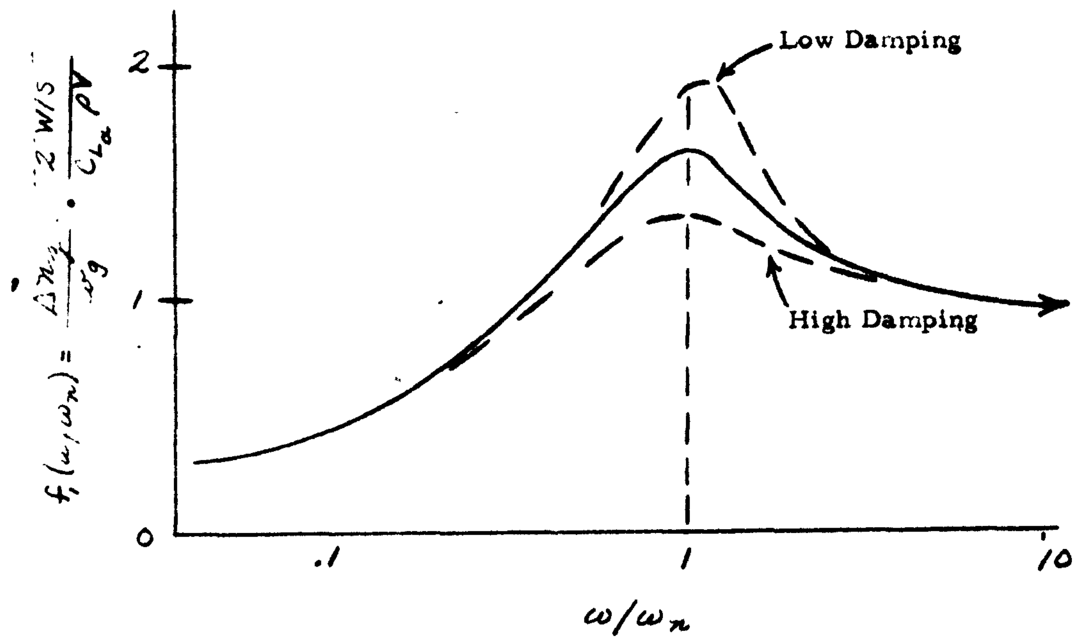

FIGURE A-1 NORMALIZED GUST TRANSFER FUNCTION

Figure A-1 shows Equation A-1 plotted in a normalized or non-dimensional form. As $\omega/\omega_n \to \infty$, $f_1(\omega/\omega_n)$ approaches unity. Examination of the form of this transfer function for a number of aircraft indicates that for the majority of aircraft one can assume that the normalized transfer function is essentially invariant. Thus, one can rewrite Equation A-1 as follows:

$$\Delta n_z / w_g = \frac{C_{L_\alpha} \rho V}{2\,W/S} f_1(\omega/\omega_n) \qquad \text{A-2}$$

It is now possible to combine Equation A-2 with the gust power spectral density and obtain a generalized power spectral density for Δn_z. If the spectrum for Δn_z is integrated over all frequencies, the mean square acceleration can be obtained.

Under most flight conditions, one can assume that the power spectral density of vertical gusts is of the form:

$$\phi_{w_g} = \sigma_{w_g}^2 \; \frac{2L/\pi}{1+\left(\frac{\omega L}{V}\right)^2} \; ; \left(\frac{ft}{sec}\right)^2 \Big/ \frac{RAD}{FOOT} \qquad \text{A-3}$$

where: ϕ_{w_g} is gust power spectral density in units of $\frac{(\text{ft/sec})^2}{\text{rad/ft}}$

$\sigma_{w_g}^2$ is mean square gust velocity $(\text{ft/sec})^2$

L is a constant representing the scale of turbulence roughly proportional to altitude

ω is frequency in rad/sec

V is flight speed in ft/sec

Note that gust wavelength = $2\pi V/\omega$ in feet.

The gust spectrum as defined by Equation A-3 is shown in Figure A-2.

FIGURE A-2 NORMALIZED GUST SPECTRUM

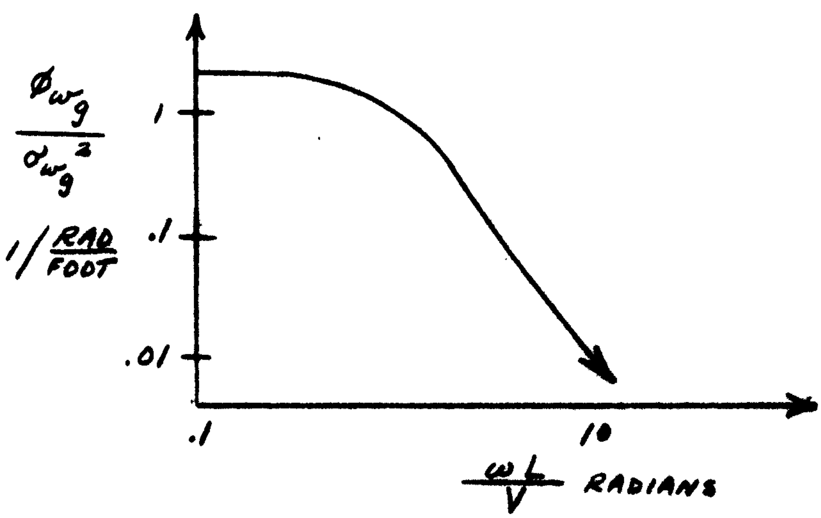

The equation relating gust spectrum to acceleration spectrum is as follows:

$$\phi_{\Delta n_z} = \left[\frac{C_{L_\alpha} \rho V}{2\, W/S}\right]^2 \left[f_1(\omega/\omega_n)\right]^2 \phi_{w_g} ; g^2 / \frac{RAD}{ft} \qquad \text{A-4}$$

Equation A-3 must be rewritten before it will be in a form compatible with Equation A-4. To convert ϕ_{w_g} to units of (ft/sec)^2 per rad/sec, we must multiply by $1/V$. The result is as follows:

$$\phi_{w_g} = \sigma_{w_g}^2 \; \frac{2L}{V} / \pi \; \frac{V^2/L^2\omega_n^2}{\frac{V^2}{\omega_n^2 L^2} + \omega^2/\omega_n^2} \; ; \; \frac{(ft/sec)^2}{RAD/SEC} \qquad \text{A-5}$$

It would be desirable to extract from Equation A-5 a function of ω/ω_n as was done with Equation A-1. For the purpose of concern here, that is, estimating the mean square acceleration by integrating Equation A-4, we can make the following approximations. For high speed low altitude flight, assume $L \approx$ 500 feet and therefore approximate V/L by 2 sec^{-1}. Approximate ω_n by 5 radians per second. Thus, Equation A-5 becomes

$$\phi_{w_g} \approx \sigma_{w_g}^2 \; \frac{1}{\pi} \; \frac{(2/5)^2}{(2/5)^2 + (\omega/\omega_n)^2} \; ; \; \frac{(ft/sec)^2}{RAD/SEC} \qquad \text{A-6}$$

$$\phi_{w_g} \approx \sigma_{w_g}^2 \; f_2(\omega/\omega_n)$$

where $f_2(\omega/\omega_n)$ varies only with ω/ω_n according to:

$$f_2(\omega/\omega_n) \approx \frac{1}{\pi} \; \frac{.16}{.16 + (\omega/\omega_n)^2} \; ; \; 1 \Big/ \frac{RAD}{SEC} \qquad \text{A-7}$$

Now we can substitute into Equation A-4.

$$\phi_{\Delta n_z} = \left[\frac{C_{L_\alpha} \rho V}{2\,W/S}\right]^2 \left[f_1(\omega/\omega_n)\right]^2 \sigma_{w_g}^2 \; f_2(\omega/\omega_n) ; \; g^2 \Big/ \frac{RAD}{SEC} \qquad \text{A-8}$$

Since $\frac{C_{L_\alpha} \rho V}{2\,W/S}$, ω_n and $\sigma_{w_g}^2$ are constants, we can integrate Equation A-8 to obtain $\sigma_{\Delta n_z}^2$.

$$\sigma_{\Delta n_z}^2 = \int_0^\infty \phi_{\Delta n_z} \, d\omega \; ; \; g^2$$

$$\frac{\sigma_{\Delta n_z}^2}{\sigma_{w_g}^2} \; \left[\frac{C_{L_\alpha} \rho V}{2\,W/S}\right]^2 \omega_n \int_0^\infty \left[f_1(\omega/\omega_n)\right]^2 f_2(\omega/\omega_n) \frac{d\omega}{\omega_n} \; ; \; g^2/(ft/sec)^2$$

Let us define $S_1 = \sigma_{\Delta n_z}/\sigma_{w_g}$ in g's/ft/sec. The product $\omega_n \left[f_1(\omega/\omega_n)\right]^2 f_2(\omega/\omega_n)$ decreases as $1/(\omega/\omega_n)^6$ for large ω/ω_n, hence the product is integrable.

The result will be some constant K_1^2 .

$$K_1^2 = \omega_n \int_0^\infty \left[f_1(\omega/\omega_n)\right]^2 f_2(\omega/\omega_n)\, d\,\omega/\omega_n \qquad \text{A-9}$$

Hence we can write:

$$S_1 = \frac{C_{L_\alpha} \rho V}{2W/S} K_1 \quad \text{IN } g's/\tfrac{ft}{sec} \qquad \text{A-10}$$

Let us examine K_1 in more detail.

$$K_1^2 = \omega_n \int_0^\infty \left[f_1(\omega/\omega_n)\right]^2 \frac{2L}{\pi V} \frac{V^2/\omega_n^2 L^2}{\frac{V^2}{\omega_n^2 L^2} + \frac{\omega^2}{\omega_n^2}}\, d\,\omega/\omega_n \qquad \text{A-11}$$

If we let $V/L\omega_n = b$, we can write Equation A-11 as follows:

$$K_1^2 = \int_0^\infty \left[f_1(\omega/\omega_n)\right]^2 2/\pi \frac{b}{b^2 + \omega^2/\omega_n^2}\, d(\omega/\omega_n) \qquad \text{A-12}$$

How does K_1^2 vary with b ? For transonic speeds at low altitudes, b is of the order .40. For this flight condition the primary contribution to the integral comes from ω/ω_n greater than 0.7. Therefore, it is possible to make a further approximation to the effect that $\omega^2/\omega_n^2 > b^2$ and modify Equation A-12 to read:

$$K_1^2 = \int_0^\infty \left[f_1(\omega/\omega_n)\right]^2 \frac{2}{\pi} \frac{b}{\omega^2/\omega_n^2}\, d(\omega/\omega_n) \qquad \text{A-13}$$

Since $2b/\pi$ does not vary with ω/ω_n, we can bring it out from under the integral sign and we can then say that

$$K_1^2 = 2b/\pi \int_0^\infty f_3(\omega/\omega_n)\, d\,\omega/\omega_n \qquad \text{A-14}$$

where $f_3(\omega/\omega_n) = \left[f_1(\omega/\omega_n)\right]^2 \frac{1}{\omega^2/\omega_n^2}$

Since the integral is a constant, we can say that K_1^2 is proportional to $2b/\pi$ or

$$K_1 \backsim \sqrt{\frac{2V}{L\omega_n \pi}} \qquad \text{A-15}$$

From Equation A-15 it is evident that for a given value of L , the constant K_1 may vary slightly with changes in $\sqrt{V/\omega_n}$. However, it is interesting to note that for many aircraft V/ω_n is a constant in the subsonic speed range.

Perhaps the best way to illustrate how K_1 varies for different aircraft flying at high subsonic Mach No. and at low altitudes is to say that $K_1 \backsim \sqrt{1/\omega_n}$. Comparison of numerical data for a few typical aircraft indicates that K_1 can be approximated by the equation

$$\text{at the cg, } K_1 \cong .6\sqrt{5/\omega_n} \quad \text{at } M = .6 \qquad \text{A-16}$$

For high speed fighter type aircraft at M = .9 and h = 500 feet, K_1 is about .60; while for large high speed bombers, K_1 is about .80.

In conclusion Equation A-10 represents a convenient way to represent the gust sensitivity of different aircraft for comparison purposes. For high speed, low altitude flight it provides good accuracy provided that K_1 is adjusted for the value of ω_n of each aircraft under consideration.

APPENDIX B

HUMAN TOLERANCE BOUNDARIES TO VIBRATION

Much of the research on the tolerance to vibration of human beings has been performed with sinusoidal shake tables or vibrators. References 16 and 18 summarize much of the data. A summary of German research is presented in SAE Paper 310C-1961. The results show a wide spread in the tolerance and indicate that for sinusoidal oscillations at a frequency of one cycle/sec the human can tolerate, for several minutes, rms values of acceleration ranging from less than 0.10 g to somewhat more than 1.0 g. A central value might be chosen as .50 g. The individual experiments vary considerably as to the seat construction, harness and seat belt arrangements and cushioning. It is probable that in no case was the subject asked to perform typical piloting tasks including navigation while under these tests.

During the past few years a small number of random vibration programs have been performed. Some means for correlating results among the various random programs would be desirable, but to the author's knowledge is as yet unavailable. The following paragraphs outline an attempt to obtain some correlation between sinusoidal test data and flight test results.

Assume that a central value of .5 rms g represents a human tolerance boundary for sinusoidal oscillations at a frequency of one cycle/sec. How can this tolerance boundary be related to that corresponding to random vibration? It seems plausible that if random white noise is passed through a sharply resonant filter the effects upon a human vibrated by such a system would differ very little from the effects of vibration with a purely sinusoidal motion having a frequency equal to the resonant frequency of the random noise filter. It is true that the vibration amplitude would vary in the random case and the phasing of the motion would also vary; however, these variations may have a small effect upon fatigue build up. Figure B-1 shows what the time history of a filtered random noise signal might look like. Figure B-2 shows the power spectra of a filtered random noise signal and of a typical aircraft response to turbulence.

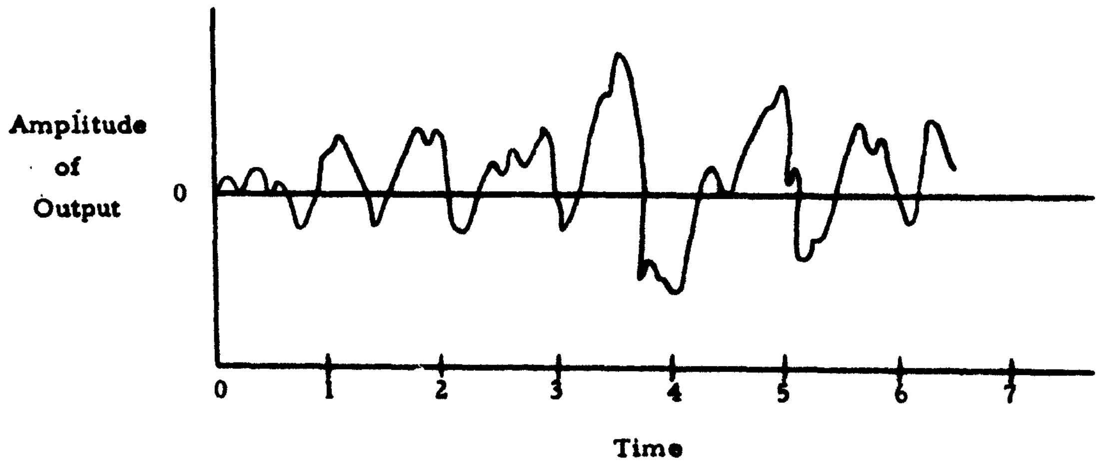

FIGURE B-1 REPRESENTATIVE TIME HISTORY OF RANDOM OUTPUT FROM LIGHTLY DAMPED SYSTEM RESONANT AT 1 CPS

If one examines the time history and power spectral density of vertical acceleration at the cockpit of an aircraft flying through turbulent air, the curves do not differ much from those shown in Figures B-1 and B-2. This is especially so if the aircraft has a short period resonant pitch mode which is poorly damped.

On the basis of this similarity we might assume that the rms tolerance boundary for sinusoidal and random processes are similar when the random process has a sharp resonant peak. If such is the case, we can say that an rms value of .5 g at a predominant frequency of one cycle/sec is the human tolerance limit after several minutes.

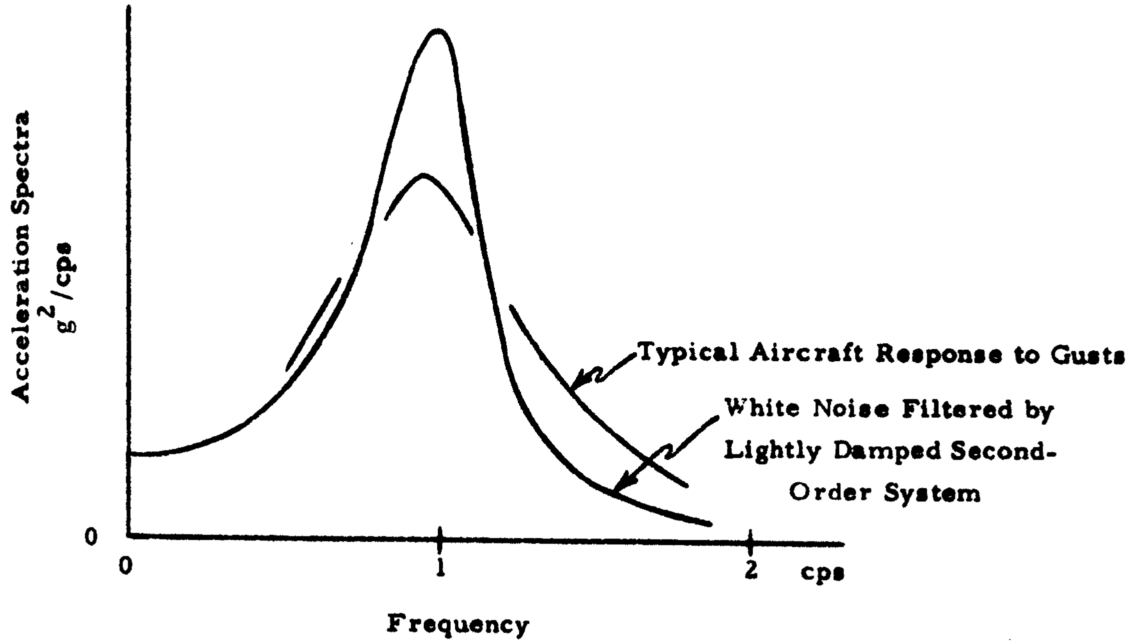

FIGURE B-2 POWER SPECTRA OF FILTERED NOISE AND AIRCRAFT RESPONSE

A comparison of data from References 4, 5, and 11 seems to indicate that a pilot would rate an rms g level of .5, which implies occasional peak incremental accelerations of 2.0 g, as intolerable after several minutes of exposure.

The foregoing indicates that very rough comparisons of a large amount of sinusoidal vibration data and a small amount of flight data do not disagree markedly in tolerance limit even though the pilot tasks and responsibilities during low level flight were considerably more complex than those for much of the sinusoidal data.

APPENDIX C

ON THE PROBABILITY OF ENCOUNTERING TURBULENCE

Data from Reference 4 was analyzed to obtain the relationship between the extreme gust peaks and the rms gust velocity contained in individual data runs. About 40 data runs ranging from 21 to 30 miles in length and averaging 26 miles in length were used in this analysis. These runs were a representative sampling of all data runs made during the B-66 program. The true rms vertical gust velocity, σ_{w_g}, was obtained from direct measurement of gust velocity and presented in Table 7 of Reference 4. The peak gust data was obtained from peak counts tabulated in Tables 8 and 11. The peak gust magnitudes for each data run were normalized by dividing by the rms for that run and plots were made of the number of peaks per mile exceeding various values of normalized gust magnitude. Such plots were made both for true vertical gust velocity, w_g, divided by σ_{w_g} and for derived vertical gust velocity, U_{de}, divided by σ_{w_g}.

The results for w_g/σ_{w_g} and for U_{de}/σ_{w_g} agreed closely with each other. For most of the runs the flight speed was 600 ft/sec and the altitude was 600 feet or less above the terrain. Some runs were made at 1,000 feet. The majority of runs contained at least one peak gust exceeding three times the rms value, 3 σ_{w_g}. Non-homogeneities were indicated in about 15% of the runs by the presence of one peak exceeding 5 σ_{w_g}. The distribution was such that one peak which exceeded 4 σ_{w_g} occurred every 10 miles. The peak variation for 35 of the runs was between 3.4 σ_{w_g} to 5.0 σ_{w_g}.

Thus one may conclude that for individual runs through turbulent air, runs of 10 to 25 miles in length, the peak gust encountered once per 10 miles will be four times the rms value of the sample run.

In constructing a model of turbulence which assumes that the turbulence is composed of patches 10 miles in length, the big question which arises is how does one cumulate patches. In other words, if we choose 10,000 miles as a reasonable sample length, Figure 4 indicates that we will on the average find one peak exceeding 33 fps, 10 peaks exceeding 26 fps and 100 peaks exceeding 20 fps. One might assign these peaks to patches in any number of different ways. For example consider that one patch with $\sigma_{w_g} \leq$ 8-1/3 fps may contain 20 peaks of $U_{de} \geq$ 20 fps.

Therefore, we must then say that 20 of the 100 peaks exceeding 20 fps are accounted for by the one patch having $\sigma_{w_g} \leq$ 8-1/3. What are the σ_{w_g} values of the patches which contribute the other 80 peaks?

The model of turbulence described herein can be used to estimate the number of patches of various σ_{w_g} values contained in a large sample of turbulence by using an approach similar to that of Reference 7. However, if only short distances in any one flight are critical for design purposes and if one assumes (quite reasonably at low altitudes) that one 10 mile patch of severe turbulence will not exist surrounded by still air, but will be surrounded by several patches of turbulence of similar intensity, then the model described herein can be used as a quick means for predicting probabilities. If the NACA data shown in Figure 5 is corrected for the inaccuracies in $\overline{A}_1$, it tends to agree with the curve identified by triangles shown in Figure 5.

Note that the curve identified with triangles does not extend down to very low values of σ_{w_g}. This curve was terminated thusly to indicate that the model used loses accuracy in representing the process at low values of σ_{w_g}.

In other words, the model described herein should be used only to estimate probabilities related to the extreme conditions or large σ_{w_g} which are associated with small probabilities.

Considerable work remains to be done so that a workable model can be obtained which will enable one to take into account the relationship of the intensity levels among adjacent turbulence patches, the extent of such relationships (100, 200 or 500 miles?) and also to take into account the relationship between adjacent patches of varying σ_{w_g} levels (how do we cumulate over σ_{w_g} and over space?).

The model described in Reference 7 does not provide data on these interrelationships. The main reason for this is that peak count data for many flights is lumped together into one probability distribution. Thus, the interrelationships between adjacent intensity levels and patches adjacent in space is lost.

When considering problems which involve 10 to 20 patches (100 to 200 miles), it is important that the interrelationships be considered. This can be done for design purposes to some extent if one applies the probabilities to missions rather than individual 10 mile patches. In other words, as discussed in the text, one should say one out of 7 missions will be performed in turbulence of $\sigma_{w_g} \geqq 5$ rather than one out of every 7 patches in a given mission.